

Change of microstructure of polyimide thin films under the action of supercritical carbon dioxide and its influence on the transport properties

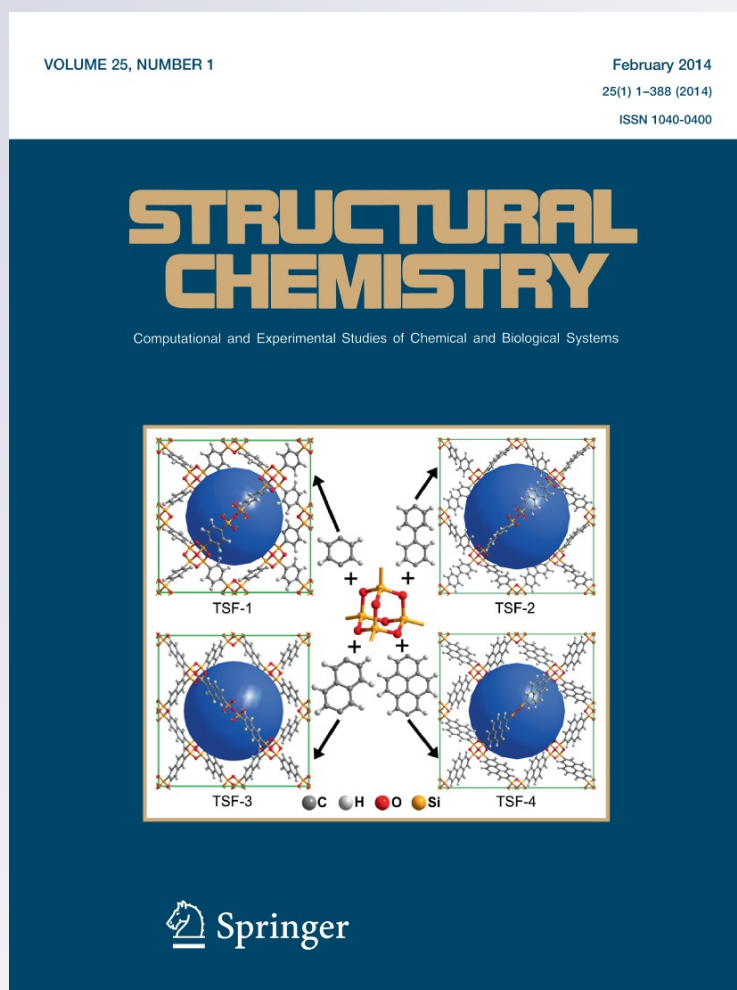
**I. A. Ronova, A. Yu. Alentiev, S. Chisca,
I. Sava, M. Bruma, A. Yu. Nikolaev,
N. A. Belov & M. I. Buzin**

Structural Chemistry

Computational and Experimental
Studies of Chemical and Biological
Systems

ISSN 1040-0400
Volume 25
Number 1

Struct Chem (2014) 25:301-310
DOI 10.1007/s11224-013-0282-5



Your article is protected by copyright and all rights are held exclusively by Springer Science +Business Media New York. This e-offprint is for personal use only and shall not be self-archived in electronic repositories. If you wish to self-archive your article, please use the accepted manuscript version for posting on your own website. You may further deposit the accepted manuscript version in any repository, provided it is only made publicly available 12 months after official publication or later and provided acknowledgement is given to the original source of publication and a link is inserted to the published article on Springer's website. The link must be accompanied by the following text: "The final publication is available at link.springer.com".

Change of microstructure of polyimide thin films under the action of supercritical carbon dioxide and its influence on the transport properties

I. A. Ronova · A. Yu. Alentiev · S. Chisca ·
I. Sava · M. Bruma · A. Yu. Nikolaev ·
N. A. Belov · M. I. Buzin

Received: 11 March 2013 / Accepted: 28 April 2013 / Published online: 31 May 2013
© Springer Science+Business Media New York 2013

Abstract Thin films of four polyimides of various structures having ether, isopropylidene or hexafluoroisopropylidene groups in their repeating units, which had been synthesized in *meta*-cresol, were treated with supercritical carbon dioxide and their gas transport properties, were investigated. Transport parameters, (permeability and selectivity coefficients) measured before and after treatment with supercritical carbon dioxide, increased from 16 to 168 % and from 5 to 49 %, respectively.

Keywords Polyimides · Transport parameters · Supercritical carbon dioxide · Change of microstructure

Introduction

The widespread use of polymeric membrane materials in many areas of science and technology has stimulated the study of new polymers as potential candidates for gas transport membranes. Such studies are often conducted to find materials that are capable of operating in harsh conditions such as elevated temperature, high pressure, etc.

Most of the research devoted to the development of high performance polymers for gas separation application has focused on the variation of chemical structure to obtain novel polymers with both high permeability and high selectivity [1]. Since a typical reverse relationship between permeability and selectivity exists to make membrane separation more competitive, an important aim of polymeric membranes design is to develop materials which have both high permeability and selectivity. For such a purpose, glassy polymers are used. Thus, various classes of polymers had been synthesized and studied for use as gas separation membranes. Among these, polyimides are in an important position, since they exhibit extraordinary high gas selectivity as well as excellent thermal and mechanical stability and film-forming ability [2, 3]. Besides, there is a broad possibility of varying the chemical structure of the repeating unit aiming to change the physical properties of polyimides, including their transport characteristics [4–7].

The main deficiency of aromatic polyimides is their insolubility and infusibility due to their aromatic structure and to some branches and crosslinks formed during their high thermal imidization process in solid state. The most known polyimide film Kapton, based on pyromellitic dianhydride and diaminodiphenylether, which was tested for gas separation membrane, proved to be more suitable for barrier application than for gas separation [8]. Numerous studies were performed with polyimides in which either pyromellitic dianhydride or the diamine partner was replaced by other monomers. All these experiments exploited the simultaneously increasing fractional free volume and hindering chain motion—two main factors influencing the transport properties. The compromise between fractional free volume and hindering backbone motions can only be followed to a certain extent: if the fractional free volume is increased without limit, then

I. A. Ronova (✉) · A. Yu. Nikolaev · M. I. Buzin
Nesmeyanov Institute of Organoelement Compounds,
Vavilov Street 28, Moscow 119991, Russia
e-mail: ron@ineos.ac.ru

A. Yu. Alentiev · N. A. Belov
Topchiev Institute of Petrochemical Synthesis,
Leninskii Prospect 29, Moscow 119991, Russia

S. Chisca · I. Sava · M. Bruma
Petru Poni Institute of Macromolecular Chemistry,
Aleea Grigore Ghica Voda 41A, 700487 Iasi, Romania

the polymer would have an open structure, and lose its ability to discriminate between penetrants of different sizes, while if rigidity is very much increased, then it becomes very difficult to find suitable solvents, and the resulting materials will be very difficult to process. For polyimides, one approach to increase the solubility and processability was the introduction of flexible linkages such as ether, or bulky units such as isopropylidene or hexafluoroisopropylidene into the polymer chain [9, 10]. However, those polyetherimides reported so far did not show enough free volume and good gas separation parameters, but permselectivity of some polyetherimides could be increased by the method of film formation because of the change of free volume distribution [11].

One way to increase the free volume of polymer matrix is by swelling with supercritical carbon dioxide (CO₂). Noticeable changes can be thus achieved by creation of micro and nanoporosity in samples without deterioration of thermal and mechanical characteristics. But, as it was shown previously, a large number of polymers of various structures did not swell or swelled insignificantly in supercritical CO₂. This behavior was explained by the fact that those studied polymers had been synthesized in *N*-methylpyrrolidone as solvent which facilitated the formation of crosslinks between the macromolecular chains, and thus, the penetration of CO₂ molecules was hindered [12–15].

In this study, our aim was to investigate structural features which influence permeabilities and selectivities for various gas separations and to examine the trade-off between gas permeability which is normally associated with reduced selectivity. Since, prediction of membrane properties in terms of polymer structure is not yet reliable, a series of polyetherimides of different structures was prepared, in *meta*-cresol as solvent, to vary their molecular packing, and segmental mobility under the action of supercritical CO₂ and their gas separation behavior before and after such treatment was studied. Four gases were used to test the transport properties of these polymer films: He, O₂, N₂, and CO₂.

Calculation methods

In order to correlate the geometry of the repeating units of polymers with transport properties, the following parameters were calculated: van der Waals volume (V_w), free volume (V_f), occupied volume (V_{occ}), accessible volume (V_{acs}), fractional accessible volume (FAV), statistical Kuhn segment (A), and characteristic ratio (C_∞).

For the calculation of accessible (V_{acc}), we consider of V_{occ} and V_w . The V_{occ} of a repeating unit is given by Eq. (1) as being the sum of the Van der Waals volume (V_w) of the repeating unit and the volume of space around this unit,

that is not accessible for a given type of molecule of gas, which is named “dead volume” (V_{dead}) (Fig. 1). It is evident that the occupied volume of a repeating unit depends on the size of the gas molecule.

$$V_{occ} = (V_w + V_{dead}) \quad (1)$$

The accessible volume of a polymer (V_{acs}) is given by Eq. (2), where $N_A = 6.02 \times 10^{23}$ is Avogadro's number, ρ is the polymer density, and M_0 is the molecular weight of the repeating unit.

$$V_{acs} = \frac{1}{\rho} - \frac{N_A \times V_{occ}}{M_0} \quad (2)$$

However, more often is used the so-called FAV, without any dimensions, which gives a better concordance with the coefficients of diffusion and of permeability, that is given by Eq. (3) [16, 17].

$$FAV = V_{acs} \times \rho \quad (3)$$

To calculate the Van der Waals and the occupied volume of the repeating unit, we used the quantum chemical method AM1 [18]. The model of the repeating unit is a set of intersecting spheres coordinates of which centers coincide with the coordinates of atoms and the radii are equal to the Van der Waals radii of the corresponding atoms, as shown in Fig. 2.

Van der Waals volume (V_w) of the repeating unit is the volume of the body of these overlapping spheres. The values of Van der Waals radii were taken from the Ref. [19]. The model of the repeating unit was placed in a box with the parameters equal to the maximum size of repeating unit. By the method, Monte Carlo designated of the number of random points m that fall into repeating unit and the total number of tests M . Their ratio is multiplied by the volume of the box, as seen in Eq. (4).

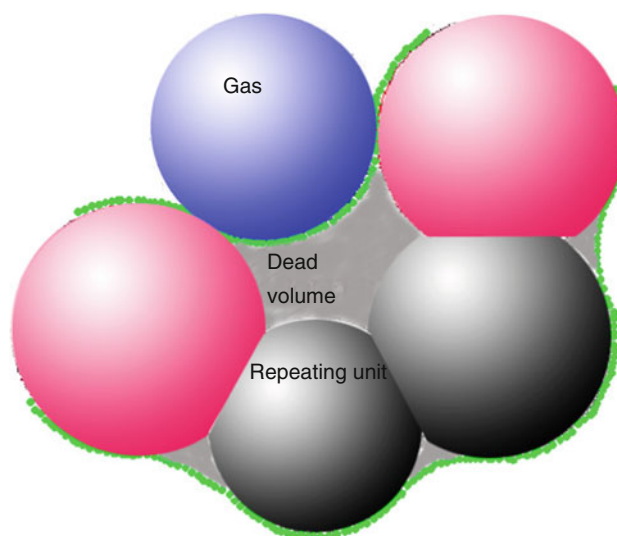


Fig. 1 The definitions dead volumes

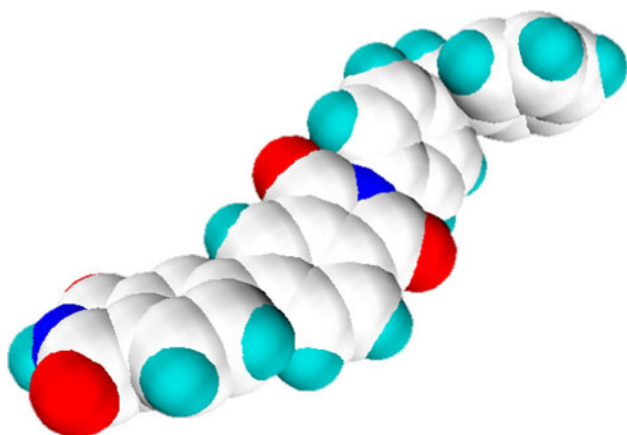


Fig. 2 View of the repeating unit with Van der Waals volume of the atoms

$$V_w = (m/M)V_{\text{box}} \quad (4)$$

Then, we calculate the dead volume. Since the molecules of O_2 , N_2 , and CO_2 have ellipsoidal shape, we calculated the dead volume of the two spheres with radii corresponding to the major and to the minor axes of the ellipsoid. A number of 10^6 spheres with the radius of the gas were generated for each atom of the repeating unit. The result is a system consisting of a repeating unit, surrounded by overlapping spheres of gas. Then, the system is placed in the “box”, similar to the one used in the determination of V_w , and random points are generated in the volume of the box [20, 21]. Thus, without making any assumptions about packing of the polymer chains in the glassy state, we can quickly calculate the Van der Waals volume, and the occupied and the accessible volumes.

The V_f was calculated with the Eq. (5):

$$V_f = \frac{1}{\rho} - \frac{N_A \times V_w}{M_0} \quad (5)$$

The value V_f , thus calculated, shows the volume which is not occupied by the macromolecules in 1 cm^3 of polymer film.

Another parameter which we calculated was statistical Kuhn segment A_{fr} . This parameter was calculated under the assumption of free rotation by using Eq. (6):

$$A_{fr} = \lim_{n \rightarrow \infty} \left(\frac{\langle R^2 \rangle}{nl_0} \right) \quad (6)$$

where $\langle R^2 \rangle/nl_0$ is the ratio of the average square end-to-end distance of a chain to its contour length ($L = nl_0$ is a parameter independent of the chain conformation); n is the number of repeating units; and l_0 is the contour length of a repeating unit [22, 23]. In the case of polyheteroarylenes, in which the repeating unit contains virtual bonds with different lengths and different angles between them, l_0 is the length of the zig-zag line connecting the midpoints of

the virtual bonds. The Kuhn segment length was calculated by Monte Carlo method.

Since in our case, the repeating units have isopropylidene or hexafluoroisopropylidene groups, it is necessary to consider their influence on the free rotation around the nearest virtual links. The rotation in this case is hindered. The calculation of the hindrance of rotation was performed by using the method described in this article [24].

Another parameter of conformational rigidity is named characteristic ratio C_∞ , and it shows the number of repeating units in Kuhn segment, as shown in Eq. (7):

$$C_\infty = \frac{A}{l_0} \quad (7)$$

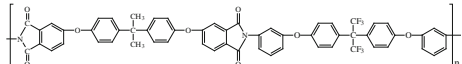
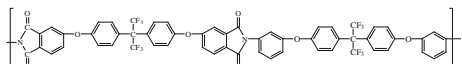
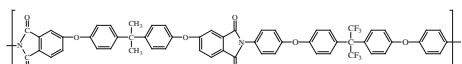
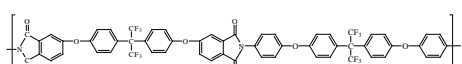
Experimental methods

Preparation of polymer films

A series of polyimides of which the structures shown in Table 1 was synthesized by polycondensation reaction of an aromatic diamine with an aromatic dianhydride by traditional method using *meta*-cresol as solvent [25], at high temperature to allow the complete imidization process and exclude of crosslinking. The monomers were selected in such a way that both of the reaction partners contained a flexible linkage such as ether, isopropylidene, or hexafluoroisopropylidene, which were expected to provide a good solubility of the resulting polymers. Thus, the selected diamines were: bis(*m*-aminophenoxy-*p*-phenylene)-hexafluoroisopropane and bis(*p*-aminophenoxy-*p*-phenylene)-hexafluoroisopropane; the dianhydrides were: isopropylidene-diphenoxy-bis(phthalic-anhydride) and hexafluoroisopropylidene-diphenoxy-bis(phthalic anhydride). The polycondensation reaction was run with equimolar quantities of diamine and dianhydride, at room temperature for 3 h, and then at 200 °C for another 7 h. After cooling down to room temperature, the resulting viscous solution was poured in methanol to precipitate the polymer. The fibrous precipitate was washed with methanol and dried in vacuum oven at 100 °C. These polymers showed good solubility in common solvents, having low boiling point, such as chloroform and tetrahydrofuran, which are very convenient for film preparation.

Weight-average molecular weights (M_w) and number-average molecular weights (M_n) of these polymers were determined by means of gel permeation chromatography (GPC) using a Waters GPC apparatus, provided with refraction and photodiode array detectors and Phenomenex-Phenogel MXN column. Measurements were carried out with polymer solutions having 0.2 % concentration, using tetrahydrofuran as eluent. Polystyrene standards of known molecular weight were used for calibration. The

Table 1 Structures of the repeating unit, molecular weight values and conformational parameters of polymers

Polymer	Repeating unit	Mw (g/mol)	Mn (g/mol)	Mw/ Mn	<i>l</i> (Å)	<i>A_h</i> (Å)	<i>C_∞</i>	<i>M₀</i>	<i>V_w</i> (Å) ³
1		66,700	46,300	1.44	41.86	20.28	0.484	1,002.93	854.488
2		44,100	34,000	1.29	41.86	21.71	0.495	1,110.87	877.824
3		96,700	65,800	1.46	42.03	27.17	0.596	1,002.93	854.488
4		43,600	33,500	1.30	42.03	27.75	0.650	1,110.87	877.824

values of weight-average molecular weight (Mw), number-average molecular weight (Mn), and polydispersity (Mw/Mn) are given in Table 1.

The films, having the thickness usually in the range of 20–40 μm, were prepared by using solutions of polymers in chloroform, having the concentration of 15 %, which were cast onto cellophane and heated gently to evaporate the solvent. The films were carefully taken out of the substrate and were used afterward for various measurements.

Measurement of glass transition temperature

The glass transition temperature (T_g) of the polymers was measured by differential scanning calorimetry, using a “DSC-822e” (Mettler-Toledo) apparatus, by using samples of polymer films. The samples were heated at the rate of 10 °C/min under nitrogen to above 300 °C. Heat flow versus temperature scans from the second heating run was plotted and used for reporting the T_g . The middle point of the inflection curve resulting from the second heating run was assigned as the T_g of the respective polymers. The precision of this method is ± 7 –10 °C.

Measurement of density

The density of polyimide films was measured by using the hydrostatic weighing method. The study was performed with an equipment for density measurement and an electronic analytic balance Ohaus AP 250D, precision of 10^{-5} g, from Ohaus Corp US which was connected to a computer. With this equipment, we measured the change of sample weight (density) during the experiment, with a precision of 0.001 g/cm³ in the value of density. Ethanol and isopropanol were taken as liquids with known density. The studied polyheteroarylenes did not absorb and did not

dissolve in these solvents, due to low diffusion coefficients. The characteristic diffusion times were in the domain of 10^4 – 10^5 s, even for the most thin films studied here, which leads to higher times of 1–2 order of magnitude than that of the density measurement. This is why the sorption of solvent and the swelling of the film must have only insignificant influence on the value of the measured density. All measurements of the density were performed at 23 °C. The density was calculated with the Eq. (8):

$$\rho_s = \rho_l \times W_a / (W_a - W_l) \quad (8)$$

where ρ_s is density of the sample, W_a is the weight of the sample in air, W_l is the weight of the sample in liquid, and ρ_l is the density of liquid. The error of the density measurements was 0.3–0.5 %.

Method of treatment with supercritical carbon dioxide (sc-CO₂)

The method of treatment with sc-CO₂ and the experimental set-up were described in previous articles [13, 26–28]. This experimental setup is composed of a generator which can provide CO₂ up to 35 MPa pressure (High Pressure Equipment Company, USA). A system of valves ensures the CO₂ access to the reaction cell with the volume of 20–30 cm³. The pressure generator and the reaction cell are provided with manometers to allow a control of the pressure. The temperature control allows a precision $\geq \pm 0.2$ °C. The cell is designed for experiments at pressures up to 70 MPa and temperatures up to 220 °C.

The following experimental technique was applied: the polymer film was weighed and placed into the cell. Film diameter was 46 mm and thickness measured with vertical projection optometer IKV-3 was 25–35 μm. The cell was purged with CO₂ to remove air residue and sealed. The pressure was increased up to the desired value (120 bar)

and film was exposed for 6 h at required temperature (40 °C). Then the cell was slowly decompressed at constant temperature with pressure decrease rate of 5–15 bar/h. After that film was exposed at normal conditions for 3–4 days, for residual CO₂ elimination, followed by test film weight measurement.

Measurement of transport parameters

The transport parameters at 25 ± 3 °C for He, O₂, N₂, and CO₂ were measured using a mass spectrometric technique [29, 30] and barometric techniques on a Balzers QMG 420 quadrupole mass spectrometer (Liechtenstein) MKS-Baratron [31], respectively. The upstream pressure was 0.8–0.95 atm, and the downstream pressure was about 10^{-3} mm Hg for spectrometric method, while for barometric technique that pressure was in the range of 0.1–1 mm Hg; therefore, the reverse diffusion of penetrating gas was negligible.

The permeability coefficients P were estimated using the formula: $P = J_s l / \Delta p$, where J_s (cm³ (STP)/cm² × s) is the flux of the penetrant gas through 1 cm² of the film; Δp (cm Hg) is the pressure drop on the film; l (cm) is the film thickness.

The diffusion coefficient (D) was determined by using the Daynes–Barrer (time lag) method: $D = l^2/6\theta$, where θ (s) is the time lag. The solubility coefficient S was estimated as the ratio: $S = P/D$.

Results and discussion

Table 1 shows the structures of four polyetherimides based on polycondensation reaction of an aromatic diamine, such as bis(*m*-aminophenoxy-*p*-phenylene)-hexafluoroisopropane and bis(*p*-aminophenoxy-*p*-phenylene)-hexafluoroisopropane, with an aromatic dianhydride, such as isopropylidene-diphenoxy-bis(phthalic-anhydride) and hexafluoroisopropylidene-diphenoxy-bis(phthalic anhydride). The reaction was performed in *meta*-cresol at high temperature. For these polymers, we calculated the values of Kuhn segment and the values of Van der Waals, occupied and accessible volumes, and these data are also shown in Table 1. Glass transition temperature, density, and transport parameters of the polymer films, before and after treatment with supercritical carbon dioxide, are presented in Tables 2, 3, 4, 5, and 6.

Figure 3 presents the dependence of glass transition temperature of these polymers on their conformational rigidity. It can be seen that all four points corresponding to the glass transition temperature of each polymer are located on a straight line having a high correlation coefficient,

98.89 %. This shows, on one hand, that the cyclization to imide structure was complete [32]. On another hand, it shows that with increasing of conformational rigidity, the glass transition temperature increases, because the probability of conformational transitions decreases, that was also shown for other polymer systems [33–35]. However, as seen in Table 2, the glass transition temperature of polymers 3 and 4 are very similar, although it was expected that the T_g of polymer 4 would have been higher than that of polymer 3 due to the presence of CF₃ groups in polymer 4; this behavior could be explained by the slightly higher molecular weight value of polymer 3 (Table 1). Moreover, it can be noted that the rigidity of the polymers 3 and 4 does not differ significantly, but intermolecular interactions decrease due to one-another repulsion of fluorine atoms. This results in slight decreasing of glass transition temperature of the polymer 4, although the reduction is in range of accuracy of the technique used.

As it was previously reported when studying a large number of polyheteroarylenes, the degree of swelling with sc-CO₂ depends on their conformational rigidity. The highest degree of swelling was obtained for those polymers having the value of characteristic ratio of 0.45–0.80 [36].

After treatment with sc-CO₂, all these four polymers exhibited a lower density and a higher free volume compared with the untreated samples. The highest increase of free volume was observed in case of polymer 1 containing *meta*-substituted phenylene rings in the diamine segment [11].

After swelling with sc-CO₂, the free volume of polymer matrix increases with 4–16 % (Table 2). The highest increase of free volume was observed in case of polymer 1, being 16 %. The glass transition temperature of these polymers did not change (in the range of the precision of DSC measurement). It means that the T_g of these polymers is predominantly determined by the chemical structure of the polymer chain itself.

Tables 3, 4, 5 and 6 present the permeability and diffusion coefficients through polymer films (membranes), before and after treatment with sc-CO₂. The dependences of permeability (a) and diffusion (b) on the FAV for each polymer in the system one polymer—different gases are given in Figs. 4, 5, 6, 7 (before sc-CO₂ treatment—the right-side lines described by equation $y = A + Bx$). The value of the Van der Waals radius of Helium is 1.22–1.80 Å, according to literature data [37–39]. In our calculations, we used the value of 1.22 Å for the Van der Waals radius of Helium. It came out that the point corresponding to the value of 1.22 Å clearly goes out of general dependences both of permeability coefficient and of diffusion coefficient for all four polymers. That point remains on the general dependence only in case when the Van der Waals radius of Helium is taken equal to 1.68 Å. Similar

Table 2 Change of free volume (V_f) after swelling at pressure of 120 bar and temperature of 40 °C

Polymer	Before swelling in sc-CO ₂			After swelling in sc-CO ₂			ΔV_f (cm ³ /g); (%)
	ρ (g/cm ³)	V_f (cm ³ /g)	T_g (°C)	ρ (g/cm ³)	V_f (cm ³ /g)	T_g (°C)	
1	1.389	0.2070	167	1.328	0.2400	169	0.0330; 16
2	1.431	0.2230	181	1.414	0.2314	180	0.0084; 3.8
3	1.341	0.2327	207	1.321	0.2440	206	0.0113; 4.9
4	1.428	0.2245	204	1.394	0.2416	204	0.0171; 7.6

Table 3 Change of transport parameters by swelling in supercritical carbon dioxide (sc-CO₂) of polymer film 1

Gas	Before swelling in sc-CO ₂					After swelling in sc-CO ₂					
	V_{occ} (Å ³)	V_{acs} (cm ³ /g)	1/FAV	P (Barrer)	$D \times 10^8$ (cm ² /s)	V_{acs} (cm ³ /g)	1/FAV	P (Barrer)	ΔP (%)	$D \times 10^8$ (cm ² /s)	ΔD (%)
He*	896.194	0.1819	3.957	7.57	373	0.2150	3.502	20.3	168.2	320	-14.2
He	913.653	0.1714	4.200	7.57	373	0.2045	3.682	20.3	168.2	320	-14.2
O ₂	924.118	0.1652	4.359	0.497	1.19	0.1982	3.799	1.2	141.4	0.87	-26.9
N ₂	928.424	0.1626	4.428	0.0824	0.32	0.1956	3.849	0.14	69.9	0.17	-46.0
CO ₂	917.956	0.1688	4.264	2.06	0.29	0.2019	3.729	5.4	162.1	0.27	-7.85

He*: when the Van der Waals radius of Helium atom was taken equal to 1.68 Å

Table 4 Change of transport parameters by swelling in supercritical carbon dioxide (sc-CO₂) of polymer film 2

Gas	Before swelling in sc-CO ₂					After swelling in sc-CO ₂					
	V_{occ} (Å ³)	V_{acs} (cm ³ /g)	1/FAV	P (Barrer)	$D \times 10^8$ (cm ² /s)	V_{acs} (cm ³ /g)	1/FAV	P (Barrer)	ΔP (%)	$D \times 10^8$ (cm ² /s)	ΔD (%)
He*	929.421	0.1951	3.582	16.8	869	0.2035	3.476	35.8	111.3	600	-31.0
He	948.302	0.1848	3.781	16.8	869	0.1932	3.660	35.8	111.3	600	-31.0
O ₂	959.582	0.1805	3.910	1.03	2.61	0.1889	3.743	2.7	162.1	1.7	-34.9
N ₂	965.011	0.1758	3.965	0.169	0.65	0.1842	3.840	0.4	136.7	0.40	-38.6
CO ₂	952.702	0.1824	3.831	4.13	0.64	0.1908	3.706	10.0	142.1	0.43	-33.1

He*: when the Van der Waals radius of Helium atom was taken equal to 1.68 Å

Table 5 Change of transport parameters by swelling in supercritical carbon dioxide (sc-CO₂) of polymer film 3

Gas	Before swelling in sc-CO ₂					After swelling in sc-CO ₂					
	V_{occ} (Å ³)	V_{acs} (cm ³ /g)	1/FAV	P (Barrer)	$D \times 10^8$ (cm ² /s)	V_{acs} (cm ³ /g)	1/FAV	P (Barrer)	ΔP (%)	$D \times 10^8$ (cm ² /s)	ΔD (%)
He*	921.752	0.1923	3.877	13.7	740	0.2036	3.717	25.2	83.9	200	-73.0
He	940.301	0.1812	4.115	13.7	740	0.1925	3.932	25.2	83.9	200	-73.0
O ₂	951.951	0.1742	4.280	1.09	2.44	0.1855	4.081	2.1	92.7	1.6	-34.4
N ₂	956.140	0.1717	4.343	0.185	0.67	0.1830	4.137	0.4	116.2	0.40	-40.3
CO ₂	945.712	0.1780	4.193	5.18	0.67	0.1892	4.000	8.6	66.0	0.47	-29.8

He*: when the Van der Waals radius of Helium atom was taken equal to 1.68 Å

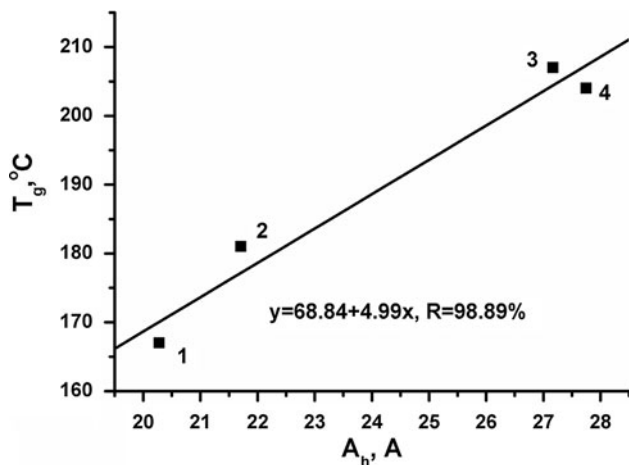
results were obtained for Helium previously [40]. The value of 1.68 Å obtained by us for the Van der Waals radius of Helium is close to the effective diameter (1.78 Å) calculated by other authors [41].

In Tables 3, 4, 5, and 6, it can be seen that after swelling with sc-CO₂, the permeability coefficients increased for different gases and different polymers from 66 to 168 %. For polymer 1, the increase of permeability coefficients of

Table 6 Change of transport parameters by swelling in supercritical carbon dioxide (sc-CO₂) of polymer film **4**

Gas	Before swelling in sc-CO ₂					After swelling in sc-CO ₂					
	V_{occ} (Å ³)	V_{acs} (cm ³ /g)	1/FAV	P (Barrer)	$D \times 10^8$ (cm ³ /s)	V_{acs} (cm ³ /g)	1/FAV	P (Barrer)	ΔP (%)	$D \times 10^8$ (cm ³ /s)	ΔD (%)
He*	929.658	0.1964	3.566	13.6	521	0.2135	3.360	30.9	127.2	1008	93.5
He	948.954	0.1859	3.765	13.6	521	0.2030	3.533	30.9	127.2	1008	93.5
O ₂	960.356	0.1798	3.896	1.03	2.67	0.1968	3.644	2.4	133.0	1.8	-3.6
N ₂	964.170	0.1777	3.951	0.189	0.71	0.1948	3.683	0.5	164.6	0.50	-29.6
CO ₂	953.666	0.1834	3.812	4.72	0.71	0.2005	3.578	11.1	135.2	0.66	-7.2

He*: when the Van der Waals radius of Helium atom was taken equal to 1.68 Å

**Fig. 3** Dependence of glass transition temperature (T_g) on Kuhn segment (A)

He, O₂, and CO₂ is higher than that of N₂. The diffusion coefficients decreased from 7.2 to 93 % with exception He of polymer 4. The change of D should be evidently observed for He, although the error of $D(\text{He})$ is quite high due to short the time lag (~ 0.5 s). And only for $D(\text{He})$ in polymer 4 increasing after treating in sc-CO₂ was observed. It is interesting that for O₂ and N₂, the diffusion decreases for all polymers in a similar way, with 27–35 and 37–46 %, respectively. The minimum change of diffusion coefficient of CO₂ was observed in case of polymers **1** and

4, by comparison with polymers **2** and **3**. For polymers **1** and **4**, the decrease of diffusion coefficient D for CO₂ is of 7 %, while for polymers **2** and **3**, it decreased with 30 %. It can be seen that the increase of free volume of polymers **1** and **4** (Tables **3** and **6**) is significantly higher than that of polymers **2** and **3** (Tables **4** and **5**).

The behavior when diffusion coefficient decreases as free volume in a polymer increases is not conventional. According to so-called “hole-wall” model [42], diffusion selectivity is a measure of density or ordering of chain packing in “holes.” For instance, O₂/N₂ diffusion selectivity is increased for swollen polymers **1** (from 3.8 to 5.1), **2** (from 4.0 to 4.9), **3** (from 3.6 to 4.3), **4** (from 3.8 to 3.9). Thus, swelling of the polymers in sc-CO₂ results in densification of macromolecular chain packing in “walls” and the “walls” become more selective to gas transport. Similar effects were observed for behavior of gas transport parameters in “strain aged” polymer **1** films [11]. Here, increasing of permselectivity of gas pairs was observed while free volume in the polymers and ordering of polymer **1** chain packing in “walls” increased. However, in our case (in contrary to [11]), increasing of selectivity is coupled with significant growing of free volume, and “hole” sizes, respectively, that results in growing of solubility coefficients (Table 7). It seems that the increase of free volume due to swelling in sc-CO₂ is not associated with disturbed packing of macromolecular chains in polymer matrix

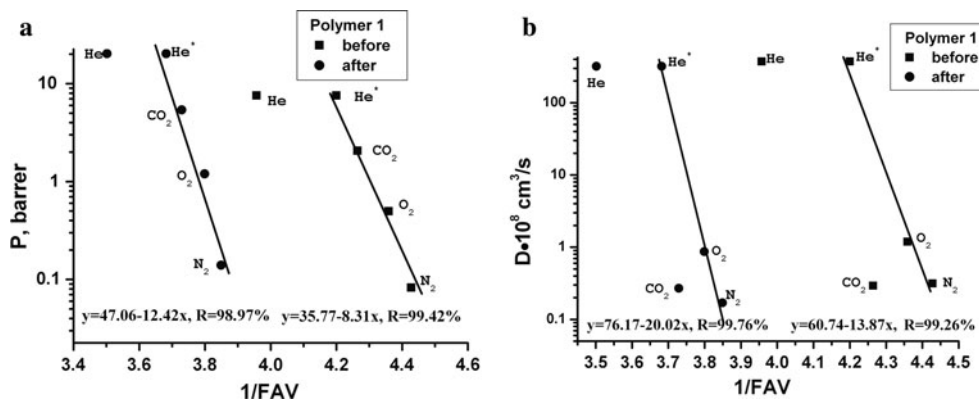
Fig. 4 Dependence of permeability coefficients, P (a) and diffusion coefficients, D (b) on the fractional accessible volume (FAV) for polymer **1**. (He*: when the Van der Waals radius of Helium atom was taken equal to 1.68 Å)

Fig. 5 Dependence of permeability coefficients, P (a) and diffusion coefficients, D (b) on the fractional accessible volume (FAV) for polymer 2. (He*: when the Van der Waals radius of Helium atom was taken equal to 1.68 Å)

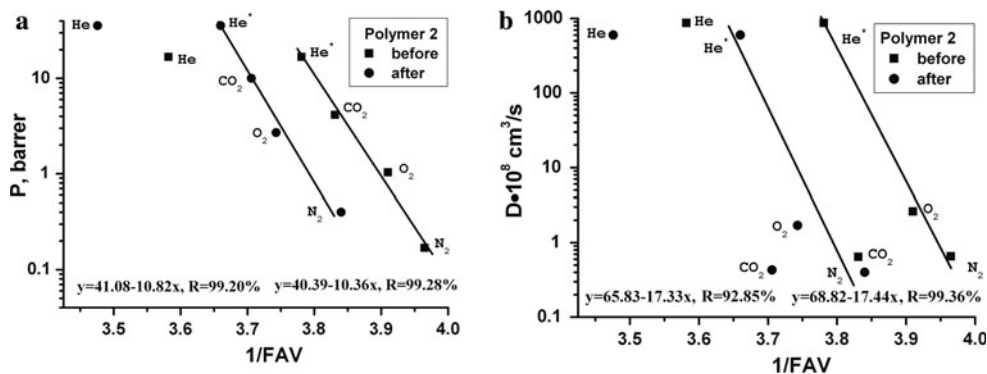


Fig. 6 Dependence of permeability coefficients, P (a) and diffusion coefficients, D (b) on the fractional accessible volume (FAV) for polymer 3. (He*: when the Van der Waals radius of Helium atom was taken equal to 1.68 Å)

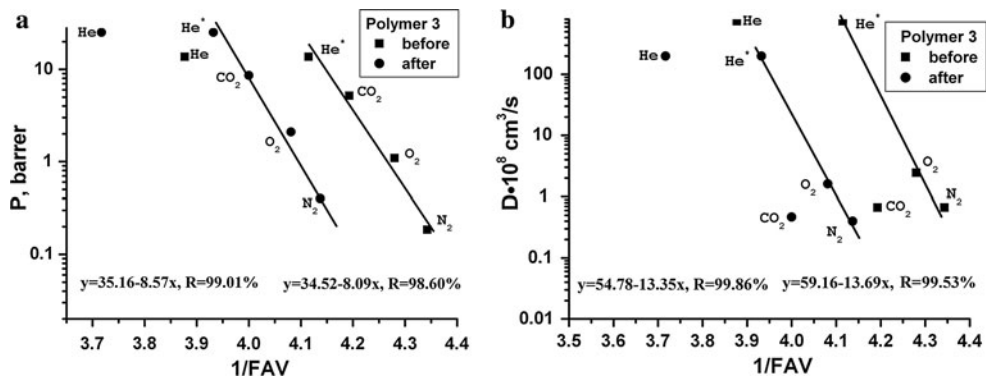


Fig. 7 Dependence of permeability coefficients, P (a) and diffusion coefficients, D (b) on the fractional accessible volume (FAV) for polymer 4. (He*: when the Van der Waals radius of Helium atom was taken equal to 1.68 Å)

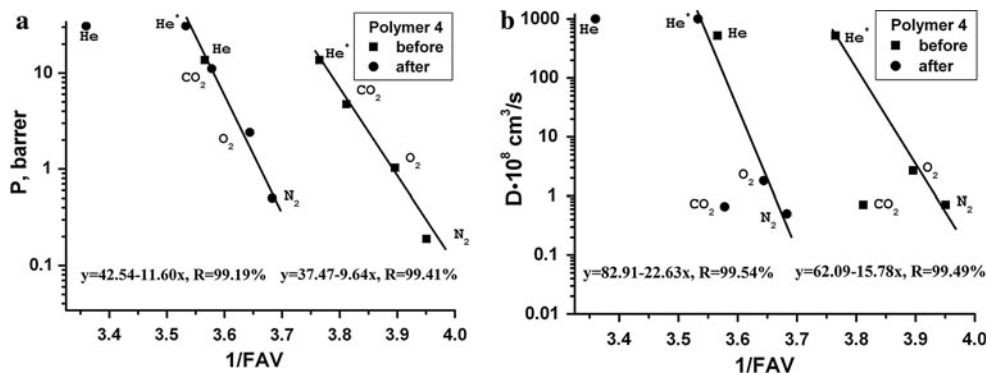


Table 7 Solubility ($S \times 10^2$, cm³(STP)/cm³ cm Hg) of gases in polymer films before and after swelling in sc-CO₂

Gas	Polymer 1			Polymer 2			Polymer 3			Polymer 4		
	Before	After	ΔS (%)	Before	After	ΔS (%)	Before	After	ΔS (%)	Before	After	ΔS (%)
He	0.21	0.63	200	0.20	0.60	200	0.19	1.3	584	0.26	0.31	19
O ₂	4.2	14	233	3.9	15	285	4.5	13	189	3.9	14	259
N ₂	2.6	8.2	215	2.6	11.0	323	2.8	9.7	246	2.65	11.0	315
CO ₂	70.5	200	184	65.0	230	254	77.0	180	134	66.0	170	158

between the microcavities, and it determines that the ordering of macromolecular chains leads to the decrease of diffusion coefficients.

Figures 4, 5, 6, and 7, left-side lines, show the dependence of permeability coefficients (a) and diffusion coefficients (b) on fractional accessible volume in the system

one polymer—different gases, after swelling with sc-CO₂. Table 8 presents the slope of these dependences (B) before and after swelling with sc-CO₂. This slope can be considered as general selectivity of a polymer to the studied gases. In Table 8, it can be seen that with regard to permeability coefficients, the selectivity increased for all

Table 8 Coefficients B in the dependence $P(1/FAV)$ and $D(1/FAV)$

Polymer	P (Barrer)			$D \times 10^8$ (cm ³ /s)		
	B before	B after	ΔB (%)	B before	B after	ΔB (%)
1	8.31	12.42	49.4	13.87	20.02	44.34
2	10.36	10.82	4.44	17.44	17.33	−0.63
3	8.09	8.57	5.93	13.69	13.35	−2.48
4	9.64	11.60	20.33	15.78	22.63	43.41

polymers from 4 to 49 %. With regard to diffusion coefficients, the selectivity increased for polymers **1** and **4**, but it decreased for polymers **2** and **3**. For these polymers **2** and **3**, the increase of free volume is significantly lower than in case of polymers **1** and **4** (Table 2).

To understand the reason of this behavior, we examine the solubility coefficients of these gases. The solubility coefficients S of each gas increases by swelling with sc-CO₂, that is by increasing of free volume (Table 7). For O₂, the solubility coefficients of all polymers increased with 190–285 %, for CO₂ they increased with 134–254 %, and for N₂ they increased with 215–323 %, which shows that they increase in a similar way for these three gases through all four polymers. The increase of solubility coefficients for Helium, of 19–584 %, makes an exception; the marginal values were found for polymers **3** and **4**, as it was the case of diffusion coefficients of these two polymers, which can also be connected with the errors in measuring of diffusion coefficient of this gas. Since the solubility of gases in swollen polymers always increases, it can be concluded that the volume of microcavities increases which determines the increase of free volume and, therefore, of the permeability coefficients.

The significant difference in the change of transport parameters of gases after treatment with sc-CO₂ between polymer **1** and polymers **2–4** is connected with the individual selection of the swelling conditions for each polymer: temperature, pressure, and speed of sc-CO₂ diffusion out of the polymer matrix. We used identical conditions of sc-CO₂ treatment for all the studied polymers.

Conclusions

The treatment with supercritical carbon dioxide leads in all studied polyimides to the increase of free volume of the polymer matrix. The increase of free volume takes place on the account of the increase of microcavities which is confirmed by the increase of solubility coefficients of all gases used in these experiments. The swelling with supercritical carbon dioxide leads to an ordered packing of macromolecular chains, which is confirmed by the increase of selectivity and by the decrease of diffusion coefficients of

all gases. As a result of swelling of polyimides with supercritical carbon dioxide, there is an increase of permeability coefficients and selectivity coefficients for most of gases. The most pronounced effect of the increase of free volume, permeability, and selectivity was observed for the less permeable of these polyimides—polymer **1**, which in previous studies showed the most visible increase of selectivity during aging in the presence of residual solvent [43].

Acknowledgments The financial support provided to I. Ronova, N. Belov, and A. Nikolaev under Russian Fond of Fundamental Investigation No. 13-08-00520 is gratefully acknowledged.

References

- Koros WJ, Fleming GK (1993) *J Membr Sci* 83:1
- Hergenrother PM (2003) *High Perform Polym* 15:3
- Liaw DJ, Wang KL, Huang YC, Lee KR, Lai JY, Ha CS (2012) *Prog Polym Sci* 37:907
- Pixton MR, Paul DR (1994) Relationship between structure and properties for polymers with aromatic backbones. In: Paul DR, Yampolskii Y (eds) *Polymeric gas separation membranes*. CRC Press, Boca Raton, p 83
- Ghanem BS, McKeown NB, Budd PM, Selbie JD, Fritsch D (2008) *Adv Mater* 20:2766
- Chen XY, Nik OG, Rodrigue D, Kaliaguine S (2012) *Polymer* 53:3269
- Yampolski Y (2012) *Macromolecules* 45:3298
- Koros WJ, Fleming GK, Jordan SM, Kim TH, Hoech HH (1998) *Prog Polym Sci* 13:339
- Yang CP, Yu CW (2001) *J Polym Sci A* 39:788
- Ronova IA, Rozhkov EM, Alentiev AY, Yampolskii YP (2003) *Macromol Theory Simul* 12(6):425
- Yampolskii Y, Alentiev A, Bondarenko G, Kostina Y, Heuchel M (2010) *Ind Eng Chem Res* 49:12031
- Ronova IA, Bruma M, Sava I, Nikitin LN, Sokolova EA (2009) *High Perform Polym* 21:562
- Ronova IA, Nikitin LN, Sokolova EA, Bacosca I, Sava I, Bruma M (2009) *J Macromol Sci A* 46:929
- Ronova IA, Sinityna OV, Abramchuk SS, AYU N, Chisca S, Sava I, Bruma M (2012) *J Supercrit Fluids* 70:146
- Ronova IA, Nikitin LN, Tereschenko GF, Bruma M (2012) *J Balkan Tribol Assoc* 18(3):425
- Plate NA, Yampolskii Y (1994) Relationship between structure and transport properties for high free volume polymeric materials. In: Paul DR, Yampolskii Y (eds) *Polymeric gas separation membranes*. CRC Press, Boca Raton, p 155
- Ronova IA, Bruma M (2012) *Struct Chem* 23(1):47
- Dewar MJS, Zoebisch EF, Stewart JJ, Healy EF (1985) *J Am Chem Soc* 107:3903
- Askadskii AA (2003) *Computational materials science of polymers*. Cambridge International Science Publishing, Cambridge
- Rozhkov EM, Schukin BV, Ronova IA (2003) *Central Eur J Chem (Central Eur Sci J)* 1(4):402
- Ronova IA, Bruma M, Schmidt HW (2012) *Struct Chem* 23(1): 219
- Hamciuc C, Hamciuc E, Ronova IA, Bruma M (1997) *High Perform Polym* 9(2):177
- Ronova IA (2010) *Struct Chem* 21:541
- Hamciuc C, Ronova IA, Hamciuc E, Bruma M (1998) *Angew Makromol Chem* 254:67

25. Bessonov MI, Koton MM, Kudryavtsev VV, Laius LA (1987) Polyimides: thermally stable polymers. Plenum Press, New York
26. Beckman EJ (2004) *J Supercrit Fluids* 28:121
27. Nikitin LN, Nikolaev AY, Said-Galiyev EE, Gamzazade AI, Khokhlov AR (2006) *Supercritical fluids. Theory Pract* 1:77
28. Nikitin LN, Gallyamov MO, Vinokur RA, Nikolaev AY, Said-Galiyev EE, Khokhlov AR, Jespersen HT, Schaumburg K (2003) *J Supercrit Fluids* 26:263
29. Yampol'skii YP, Novitskii EG, Durgar'yan SG (1980) *Zavod Lab* 46:256
30. Fielding R (1980) *Polymer* 21:140
31. Belov NA, Zharov AA, Shashkin AV, Shaikh MQ, Raetzke K, Yampolskii YP (2011) *J Membr Sci* 383:70
32. Hamchiuk E, Hulubei C, Bruma M, Ronova I, Sokolova E (2008) *Rev Roum Chim* 53(9):737
33. Ronova IA, Pavlova SSA (1998) *High Perform Polym* 10:309
34. Ronova IA, Bruma M (2010) *Struct Chem* 21:1013
35. Chisca S, Ronova IA, Sava I, Medvedeva V, Bruma M (2011) *Mater Plast* 48(1):38
36. Ronova IA, Bruma M, Chmutin IA, Jablokov MY, Kuznezov AA, Ryvkina NG (2012) In: *Proceedings of the XVIII international conference on high technologies in Russian industry*, Central Research Technological Institute Technomash, Moscow, p 321–329
37. Bondi A (1964) *J Phys Chem* 68:441
38. Huheey JE (1983) *Inorganic chemistry principles of structure and reactivity*. Harper & Row Publishers, New York
39. Bizerano J (1993) *Prediction of polymer properties*. Marcel Dekker, New York
40. Ronova IA, Sokolova EA, Bruma M (2008) *J Polym Sci B* 46:1868
41. Teplyakov VV, Meares P (1990) *Gas Sep Purif* 4:66
42. Alentiev AY, Yampolskii YP (2002) *J Membr Sci* 206:291
43. Alentiev A, Yablokova M, Lazareva Y, Vidyakin M, Kostina Y, Yampolskii Y, Antipov E, Rusanov A, Ronova I, Kuznetsov A, Bruma M (2008) *8th International Symposium on Polyimides High Polymers-Stepi 8 Montpellier*, 9–11 June 2008, p 447